

# Air-sweep vacuum membrane distillation using fine silicone, rubber, hollow-fiber membranes

Jingli Xu<sup>a</sup>, Michio Furuswa<sup>b</sup>, Akira Ito<sup>a\*</sup>

<sup>a</sup>*Department of Chemistry and Chemical Engineering, Niigata University, Ikarashi-2-8050, Niigata 950-21, Japan  
Tel. +81 (25) 262-6789, email: aito@eng.niigata-u.ac.jp*

<sup>b</sup>*Nagayanagi Co., Ltd., Kyoujima 1-1-1, Sumida-ku, Tokyo 131-0046, Japan*

Received 14 March 2005; accepted 17 August 2005

---

## Abstract

An air-sweep vacuum membrane distillation process can be used for water purification or the desalination of salt water. The process simply consists of a hollow-fiber membrane module and a diaphragm vacuum pump without a condenser for the water recovery or trap. The only operating parameter of the apparatus is the sweeping air flow rate. A membrane module using fine silicone, rubber, hollow-fiber membranes 40  $\mu\text{m}$  thick was used for the water recovery experiments from pure water or salt water. The experimental results were compared with that using a membrane module with porous polypropylene hollow-fiber membranes. The fine silicone rubber membrane module could produce condensed water at a rate comparable to the porous membrane module. For each membrane, the apparent permeability of the water vapor was evaluated from the results of another vacuum membrane distillation experiment. Based on the apparent permeability and a simple vapor-phase driving force model, model calculations were made that well predicted the experimental results of air-sweep membrane distillation.

*Keywords:* Membrane distillation; Hollow fiber; Silicone rubber

---

## 1. Introduction

Most countries are facing the problem of fresh water shortages. One solution is the use of membrane separation processes for seawater or surface

water. Among these techniques for desalination, membrane distillation (MD) is a promising one. The MD process has advantages of lower operating temperature and pressure, and uses a low-grade, waste or alternative energy source [1]. The advantages and limitations of the MD processes have been thoroughly summarized by Lawson

---

\*Corresponding author.

*Presented at the International Congress on Membranes and Membrane Processes (ICOM), Seoul, Korea, 21–26 August 2005.*

and Lloyd [2]. Vacuum membrane distillation (VMD) is a kind of MD process; it is an evaporative process using porous and hydrophobic membranes that physically separate the aqueous liquid feed from the gaseous permeate kept under vacuum [3]. A major disadvantage of the VMD process is degradation of hydrophobicity of the microporous membrane, which leads to direct permeation of the feed water. Based on this point, sweeping gas membrane distillation (SGMD) without vacuum operation for desalination has also been proposed [4,5]. For both the VMD and SGMD processes, a condenser must be used to recover the permeation water. This means that the process becomes complex. Most research regarding VMD has focused on VOC removal from water or air, while only a small study has been done on desalination or water treatment [6,7] in which a porous membrane was used.

This study proposes an air-sweep VMD process using a dense polymer membrane for water treatment. The leakage of feed water to the permeate side was avoided by using a dense membrane, and it is a simple process because no condenser was needed during the process. The water recovery rate of the process was demonstrated and compared to the results using a microporous hollow-fiber membrane module. To analyze the process performance, a simple model calculation was compared to the experimental results.

## 2. Experimental

### 2.1. Vacuum membrane distillation (VMD)

A porous membrane is usually applied to the VMD, and a dense membrane is used for the pervaporation (PV). In our VMD experiment, a porous Duraple membrane (Millpore), a polypropylene porous membrane (PP) and a silicone rubber dense membrane (SR) were used.

The experimental set-up is shown in Fig. 1(a). It consists of a feed pump and flat-sheet module

(membrane area, 24 cm<sup>2</sup>), a cold trap and a vacuum pump. The pressure on the permeate side,  $P_1$ , was adjusted by the vacuum pump, which was maintained at 0.3 kPa. Pure water was fed to the membrane module by a feed pump at room temperature and atmospheric pressure. A tube set in a cold trap in which the temperature was 230 K was used to collect the permeant.

### 2.2. Air-sweep VMD experiment

Two kinds of hollow-fiber membranes, dense and microporous, were used for the air-sweep VMD experiment. The dense membrane was a fine silicone rubber hollow-fiber membrane with a thickness of 40  $\mu\text{m}$ , newly developed by Nagayanagi (Japan). This module is referred to as the SR module. For comparison, a microporous hydrophobic PP membrane was also used. It was a Liqui-Cel x-50 G478 module (Celgard, USA), called the PP module. The membrane materials are the same as the PP and SR used in the VMD experiment. The specifications of the modules are given in Table 1.

The set-up of the air-sweep VMD process is shown in Fig. 1(b). It consists of a feed pump, a hollow-fiber module and a diaphragm vacuum pump. No need of a condenser makes the process simpler. The experiments were performed with pure water and a 3.5 wt% NaCl solution. The water or NaCl solution was fed to the shell side of the membrane module at room temperature (291–295 K) and atmospheric pressure. One port on the lumen side was open to the atmosphere through a needle valve to control the flow rate of the sweep air. Another port on the lumen side of the membrane module was connected to a mini-diaphragm vacuum pump (model N 84.4, KNF Neuberger, Germany), which has a performance better than a common diaphragm vacuum pump. The lumen side of the module was maintained at low vacuum of 2–12 kPa.

The sweeping air was taken from the atmosphere and passed through the lumen side of the

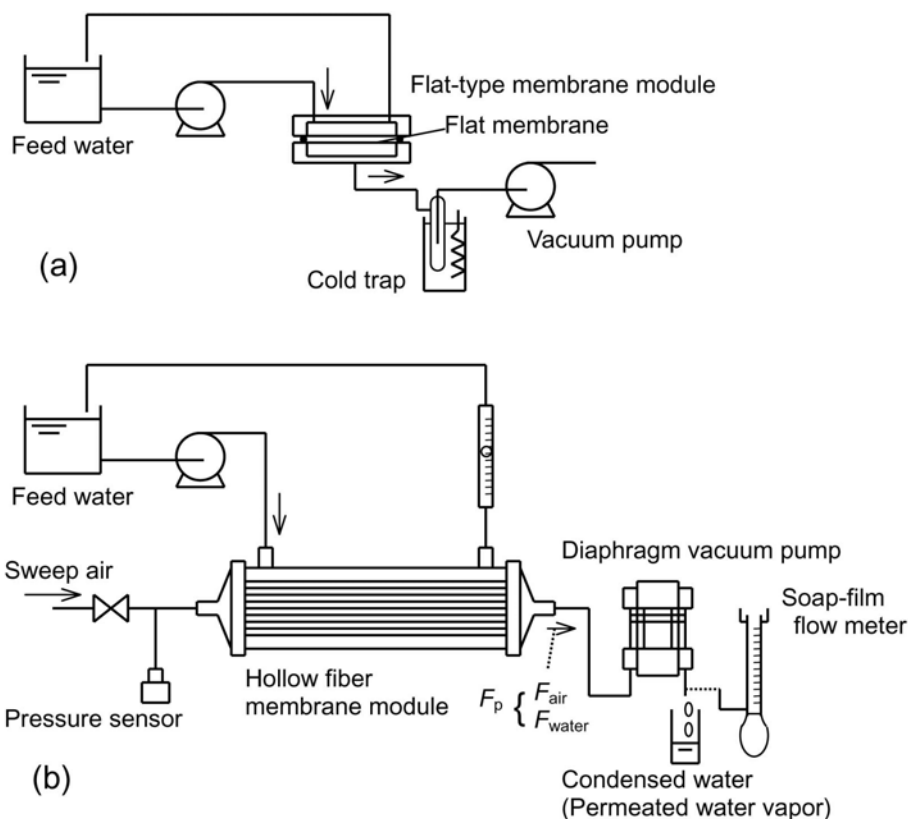


Fig. 1. Experimental apparatus for (a) VMD and (b) the air-sweep VMD.

Table 1  
Specifications of the hollow-fiber membrane modules

	Module	
	SR	PP
Membrane material	Silicone rubber	Polypropylene
Inner diameter, $\mu\text{m}$	170	220
Outer diameter, $\mu\text{m}$	250	300
Thickness of membrane wall, $\mu\text{m}$	40	40
Effective membrane length, cm	11.2	19
Membrane area, $\text{m}^2$	0.22	0.6
Mean pore size, $\mu\text{m}$		0.04
Porosity, %		40
Diameter of housing, mm	40	32
Number of fibers	3000	3600

hollow-fiber membrane. The flow rate of the sweeping air is the only operating parameter of the process. At the beginning of each run, the air flow rate was measured by a soap film flow meter. The sweeping air rate was 10–250  $\text{cm}^3/\text{min}$  of which the volume is based on atmospheric pressure and room temperature. At the outlet of the module, the sweeping air contained water vapor, which permeated through the membrane from the feed water. Ideally, the sweeping air contains water vapor at its saturation pressure. When the mixed gas, water vapor and air were released into the atmosphere at the outlet of the vacuum pump, most of the water vapor was condensed.

### 3. Results and discussion

#### 3.1. Vacuum membrane distillation (VMD)

The results of the VMD are summarized in Table 2 in order to compare the water flux from our experiment with the conventional VMD process. The PP membrane SR membranes were used in VMD. The properties of the PP membrane used in VMD were the same as the hollow-fiber used in the air-sweep VMD.

In this study, the apparent permeability of the water vapor was derived from the VMD experiments and was calculated based on the following equation:

$$Q_{\text{water}} = N_{\text{water}} \delta / (p_{\text{water}}^* - P_1) \quad (1)$$

where  $N_{\text{water}}$  is the water flux;  $\delta$  is the thickness of membrane, the difference between the water saturation vapor,  $p_{\text{water}}^*$  and the permeate pressure;  $P_1$  (0.3 kPa) is the driving force. This apparent permeability is defined by the pressure difference in the vapor and membrane thickness even for a porous membrane. In order to discuss the water flux for the VMD, PV, and air-sweep VMD on the basis of the same theoretical model, the apparent permeability of this definition was used.

For the silicone rubber dense membrane, the apparent water permeability,  $Q_{w_2}$  is  $6.63 \times 10^{-9}$  mol m/(s m<sup>2</sup> kPa) ( $1.98 \times 10^{-6}$  cm<sup>3</sup> (STP) cm/(s cm<sup>2</sup> cmHg)). This result is identical to that in our pervious report [8]. For the microporous hydrophobic membrane, the water permeability,  $Q_{w_2}$  is  $1.65 \times 10^{-7}$  mol m/(s m<sup>2</sup> kPa) ( $4.93 \times 10^{-5}$  cm<sup>3</sup> (STP) cm/(s cm<sup>2</sup> cmHg)).

#### 3.2. Air-sweep VMD

The results of the air-sweep VMD are shown in Figs. 2 and 3. Fig. 2 is the result for the pure water feed, and Fig. 3 is for the 3.5 wt% NaCl feed that represents seawater. In these figures the condensed water rate at the outlet of the pump,  $F_{\text{water}}$  [g/h], are plotted vs. the sweeping air flow rate,  $F_{\text{air}}$  [cm<sup>3</sup>/min], which is the volumetric flow rate at atmospheric pressure. In Fig. 2, the bottom figure shows the relationship between the permeate side pressure and sweeping air flow rate.

When an aqueous salt solution was used for feed, the quality of the condensed water was confirmed by the solid weight in the water. In all experiments, dry material contained in condensed water was under 0.4 mg/g-water, which means that salt concentration in the condensed water was lower than 400 ppm.

Table 2  
Experimental results for vacuum membrane distillation

Membrane	Porosity	Membrane thickness, $\mu\text{m}$	Water flux, kg/(m <sup>2</sup> ) (temperature, K)	Permeability of water vapor, $\times 10^{-6}$ mol m/(s m <sup>2</sup> kPa)
<b>This work:</b>				
Polypropylene <sup>a</sup>	Porous, 40%	25	1.15 (296)	0.165
Durapel <sup>b</sup>	Porous, 70%	98	1.45 (294)	1.17
Silicone rubber	Dense	85	0.043 (296)	0.00663
<b>PVDF [9]:</b>				
Polypropylene [10]	Porous, HF	—	0.40 (295)	
Polyethylene [11]	Porous, 76%	81	3.5 (298)	
	Porous, 53%, HF	50	1.5 (313) (salt water)	

<sup>a</sup>Flat film of 0.04  $\mu\text{m}$  pore size.

<sup>b</sup>Millipore. Modified PVDF, fluoro-monomer-treated polyvinylidene difluoride porous membrane of 0.1  $\mu\text{m}$  pore size.

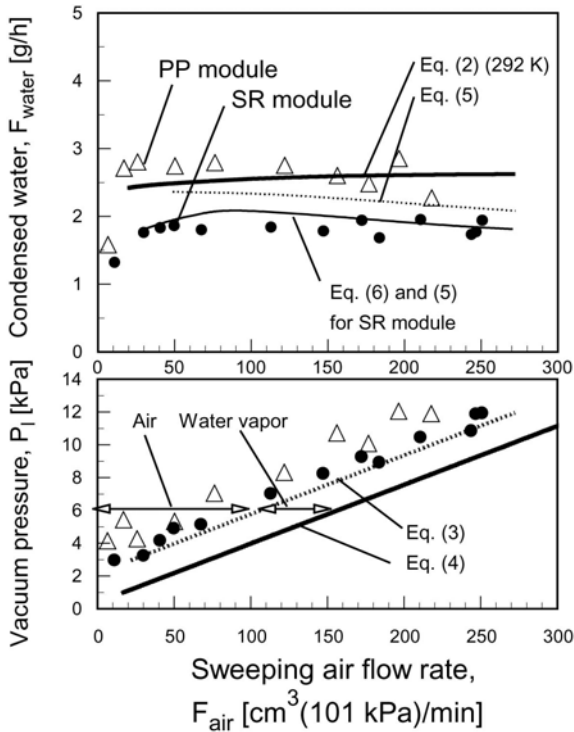


Fig. 2. Air-sweep VMD results for pure water feed.

In the upper part of Fig. 2, we can see that, for pure water feed, the condensed water rate was about 2.5 g/h for the PP module and about 2 g/h for the SR module. The fine silicone rubber membrane had a condensed water rate comparable to the microporous membrane. For the PP and SR modules, the tendencies of the condensed water rate with sweeping air rate are nearly the same. At the beginning, the condensed water rate increased with the sweeping air rate increasing to a certain value, and then it began to gradually decrease.

Assuming that the sweeping air is saturated by water vapor at the outlet of the membrane module at the vacuum pressure and all of the water vapor changed to condensed water at the outlet of the diaphragm vacuum pump, the condensing water rate can be calculated using the sweeping air flow rate according to Eqs. (2) and (3).

$$F_{\text{water}} = F_p \left( p_{\text{water}}^* / P_1 \right) \quad (2)$$

$$F_{\text{air}} = F_p \left[ \left( P_1 - p_{\text{water}}^* \right) / P_1 \right] \quad (3)$$

In this preliminary model, the contribution of water vapor accompanied with sweep air is ignored, which is 3–6% of condensed water as shown later. The calculated results from  $p_{\text{water}}^*$  at 292 K are shown by the thick line in the upper part of Fig. 2 and by the dotted line in the bottom part of Fig. 2.

The total gas flow rate,  $F_p = (F_{\text{water}} + F_{\text{air}})$ , at the outlet of the pump is related to the permeate pressure, which is dependent on the pump's performance. For the diaphragm pump used in this study, the vacuum pressure,  $P_1$ , is nearly proportional to the gas flow rate,  $F_p$ , and can be described by the performance curve of the pump, i.e., Eq. (4):

$$F_p = F_{\text{air}} + F_{\text{water}} = f(P_1) \quad (4)$$

This is shown by the solid line in the bottom part of Fig. 2. In other words,  $F_p$  is a function of  $P_1$ . The difference in the sweeping air flow rate between the pump performance, Eq. (4), and the air flow rate, Eq. (3), is the water vapor flow rate. If a pump with better performance could be used, a higher condensed water rate would be attained.

In our air sweep VMD process, the sweeping air at the outlet of the pump is not cooled, and reaches a temperature of 303 K. This means that part of the water would be removed by the sweeping air. In this situation, the condensed water rate can be calculated using Eq. (5):

$$F'_{\text{water}} = F_{\text{water}} - F_{\text{air}} \frac{p_{\text{water}, 303 \text{ K}}^*}{\pi} \quad (5)$$

This is shown in the upper part of Fig. 2 by the dotted line. Eq. (5) explains the tendency of the condensed water rate's decrease for the PP module.

Fig. 3 shows the results for the NaCl solution feed. In contrast to Fig. 2, the condensed water

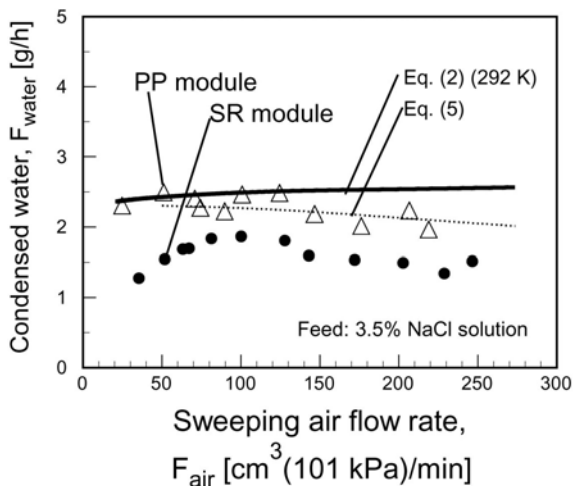


Fig. 3. Air-sweep VMD results for NaCl solution feed.

rate in Fig. 3 decreased to 80–90% of the pure water. This decrease is unexpected because the vapor pressure of the NaCl solution,  $p^*_{\text{water}}$  is only 2.2% lower than that of pure water. This decrease was mainly caused by concentration polarization. Nevertheless, the degree of decrease is relatively small. Therefore, we can say that for air sweep VMD, water flux is not dependent on the osmotic pressure of the feed water because the driving force of the process is the vapor pressure difference. The same calculation for the PP module with that for the pure water feed was also made, and the result is individually shown by the dotted line and solid line in Fig. 3.

For the SR module, the experimental data in Figs. 2 and 3 were lower than the theoretical value based on the assumption of saturated air at the outlet. This is due to the unsaturated condition of the water vapor at the outlet of the membrane module due to the low water permeability for the dense silicone rubber membrane. In this situation, a differential equation [Eq. (6)] for the water vapor flow rate along the hollow-fiber lumen was used to calculate the value.

$$\frac{dF_{\text{water}}}{dA} = \frac{Q_{\text{water}}}{\delta} \left[ p^*_{\text{water}} - P_1 \frac{F_{\text{water}}}{(F_{\text{air}} + F_{\text{water}})} \right] \quad (6)$$

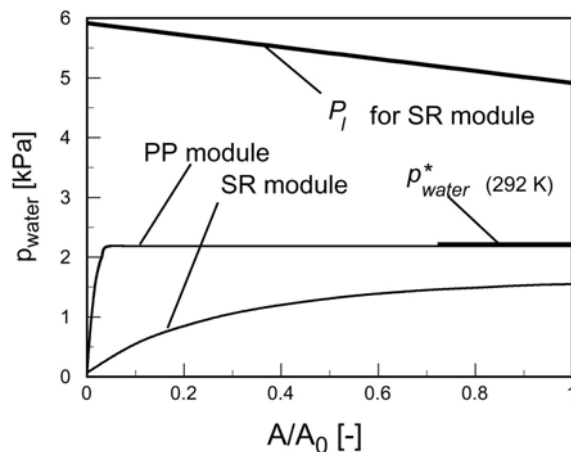


Fig. 4. Partial pressure profiles of water vapor in the membrane modules.

Initial condition:

$$F_{\text{water}} = F_{\text{water, inlet}} = F_{\text{air}} \left( \frac{p_{\text{water}}}{\pi - p_{\text{water}}} \right) \quad \text{at } A = 0$$

where  $dF_{\text{water}}$  is the water permeation rate,  $dA$  is the membrane area,  $Q_w$  is apparent permeability, and  $\delta$  is the membrane thickness. The permeate side pressure changed from the inlet to the outlet of the module. Measured values were used for this pressure drop. The initial condition means the consideration of water vapor inlet accompanied with the sweep air. The evaporation of water caused a temperature drop of the feed water. This effect is estimated by Eq. (7).

$$\frac{dT_1}{dA} = \left( \frac{dF_{\text{water}}}{dA} \right) \Delta H_v / (LC_p) \quad (7)$$

The water permeation rate was calculated by the integration of Eqs. (6) and (7) from the inlet ( $A=0$ ) to the outlet ( $A=A_0$ ) of the module. The temperature of permeate side air flow is taken to be the same as the feed water temperature because of a fine fiber diameter and the vacuum condition.

Examples of calculations are shown in Fig. 4 where the relation between the water vapor partial

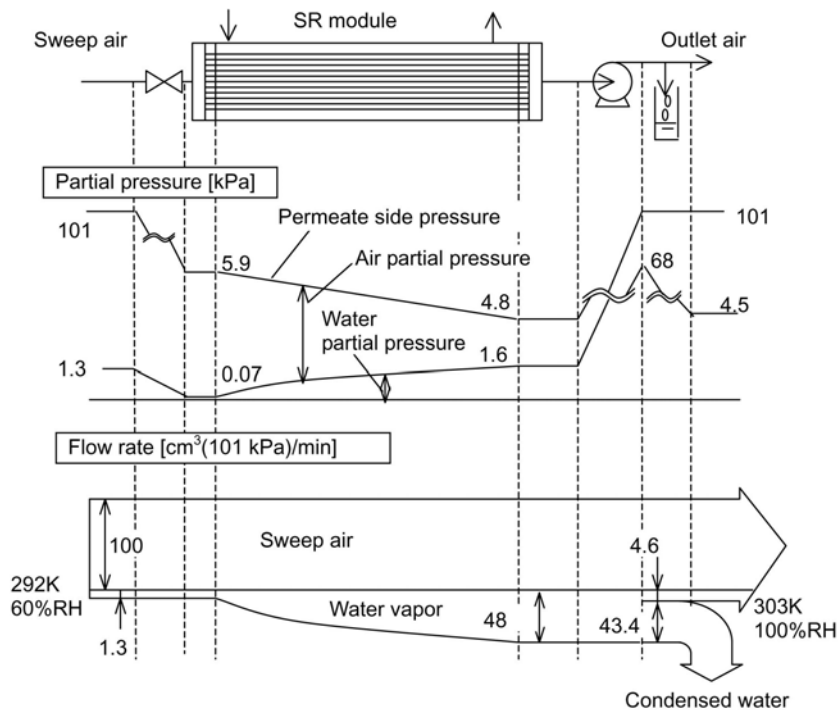


Fig. 5. Partial pressure profiles and flow rate of components in permeate side for the air-sweep VMD process using the SR module.

pressure and the membrane area is shown. For the PP module, when  $A/A_0$  is a small value, the water vapor partial pressure could almost reach the saturation vapor pressure. On the contrary, for the SR module, even if  $A/A_0$  is equal to 1, the water vapor partial pressure did not yet reach the water saturation vapor pressure. This is the reason why the condensed water rate for the SR module is lower than that for the PP module. The calculated result for the condensed water rate is shown by the thin line in the upper part of Fig. 2. It was nearly identical with the experimental results.

In the theoretical calculation the temperature drop of feed water is around 0.5 K for a 2 g/h water evaporation rate and a feed water of 50 cm<sup>3</sup>/min. The theoretical partial pressure profile and component flow rates of the permeate side in the air-sweep VMD are illustrated in Fig. 5. The conditions are the same as those in Fig. 4. The component volume flow rate is based

on atmospheric pressure. The sweep air of 100 cm<sup>3</sup>/min initially contains water vapor of 1.3 cm<sup>3</sup>/min, which is air humidity. The air carries out water vapor of 48 cm<sup>3</sup>/min at the outlet of the module. At the outlet of the vacuum pump, where the pressure returns to the atmospheric pressure, the air can contain saturated water vapor of 4.6 cm<sup>3</sup>/min at the outlet temperature. The excess water vapor of 43.4 cm<sup>3</sup>/min makes condensed water of 2.0 g-water/h.

In Fig. 6 the results of the VMD and air-sweep VMD for the pure water feed were compared. For the PP module, the water flux was about two orders of magnitude different, because in the air sweep VMD by the PP module only a small part of the membrane (5% membrane area from inlet) was used for the water recovery. For the SR module, the water flux in the air sweep VMD was about 1/4 of that in the VMD. These cause a contradiction result that the water flux per unit

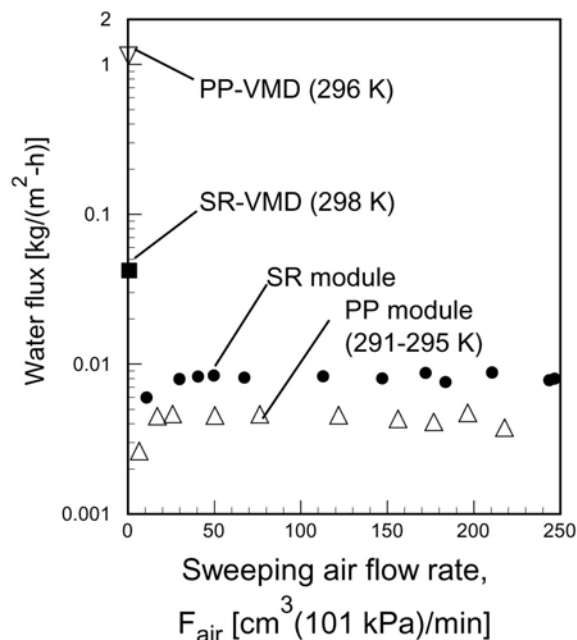


Fig. 6. Comparison of water flux.

membrane area for the SR module is larger than that of the PP module. Considering that in the air-sweep VMD process there is no need for a condenser, the air-sweep VMD using the fine dense membrane could be a promising process for water recovery.

#### 4. Conclusions

A novel air-sweep VMD process was reported for water purification or the desalination of salt water. The process simply consists of a hollow-fiber membrane module and a diaphragm vacuum pump without a condenser for the water recovery or trap. When using a dense membrane module of fine silicone, rubber, hollow-fiber membranes, leakage of the feed water to permeate side is prevented.

The experimental results were compared with that for a membrane module with PP hollow-fiber membranes. The fine silicone rubber membrane module made condensed water at a rate comparable to the porous membrane module.

For each membrane, the apparent permeability of the water vapor was evaluated from the results of another VMD experiment. Based on the apparent permeability and a simple vapor-phase driving force model, model calculations were completed, which well predicted the experimental results of the air-sweep membrane distillation.

#### 5. Symbols

- $A$  — Membrane area,  $m^2$
- $C_p$  — Heat capacity of feed water,  $J/(mol\ K)$
- $F_{water}$  — Water permeation rate in permeate side,  $mol/s$  or  $g/h$
- $F'_{water}$  — Condensed water rate,  $mol/$  or  $g/h$
- $F_p$  — Total gas rate,  $mol/s$
- $F_{air}$  — Sweeping air flow rate,  $mol/s$  or  $cm^3/min$  in dry base
- $\Delta H_v$  — Latent heat of vaporization for water,  $J/mol$
- $L$  — Feed rate of feed water,  $mol/s$
- $N_{water}$  — Water permeation flux,  $mol/(m^2\ s)$
- $p_{water}^*$  — Water saturated vapor at experimental temperature,  $kPa$
- $P_{water}$  — Water vapor partial pressure in air,  $kPa$
- $P_1$  — Permeate side pressure at the inlet of the module,  $kPa$
- $Q_w$  — Apparent permeability of water through the membrane,  $mol\ m/(s\ m^2\ kPa)$
- $T_1$  — Feed water temperature,  $K$

#### Greek

- $\pi$  — Atmosphere pressure,  $kPa$
- $\delta$  — Membrane thickness ( $m$ )

#### References

- [1] L. Martínez-Díez and F.J. Florido-Díaz, Desalination, 137 (2001) 267–273.



- [2] K.W. Lawson and D.R. Lloyd, *J. Membr. Sci.*, 124 (1997) 1–25.
- [3] C. Cabassud and D. Wirth, *Desalination*, 157 (2003) 307–314.
- [4] M. Khayet, M.P. Godino and J.I. Mengual, *Desalination*, 157 (2003) 297–305.
- [5] M. Khayet, P. Gofino and J.I. Mengual, *J. Membr. Sci.*, 165 (2000) 261–272.
- [6] A.M. Urriaga, G. Ruiz and I. Ortiz, *J. Membr. Sci.*, 165 (2000) 99–110.
- [7] N. Couffin, C. Caufin, C. Cabassud and V. Lahoussine-Iurcaud, *Desalination*, 117 (1998) 233–245.
- [8] A. Ito, Y. Feng and H. Sasaki, *J. Membr. Sci.*, 133 (1997) 95–102.
- [9] D. Wirth and C. Cabassud, *Desalination*, 147 (2002) 139–145.
- [10] K.W. Lawson and D.R. Lloyd, *J. Membr. Sci.*, 120 (1996) 111–121.
- [11] J.-M. Li, Z.-K. Xu and Z.-M. Liu, *Desalination*, 155 (2003) 153–156.